
Attributing Response to Context: A Jensen–Shannon Divergence Driven Mechanistic Study of Context Attribution in Retrieval-Augmented Generation

Ruizhe Li^{1*} Chen Chen² Yuchen Hu² Yanjun Gao⁴ Xi Wang⁵ Emine Yilmaz³

¹University of Aberdeen ²Nanyang Technological University ³University College London

⁴University of Colorado Anschutz Medical Campus ⁵University of Sheffield

Abstract

Retrieval-Augmented Generation (RAG) leverages large language models (LLMs) combined with external contexts to enhance accuracy and reliability of generated responses. However, reliably attributing generated content to specific context segments, *context attribution*, remains challenging due to computationally intensive nature of current methods, which often require extensive fine-tuning or human annotation. In this work, we introduce a novel **Jensen–Shannon Divergence** driven method to **Attribute Response to Context (ARC-JSD)**, enabling efficient and accurate identification of essential context sentences without additional fine-tuning, gradient-calculation or surrogate modelling. Evaluations on a wide range of RAG benchmarks, such as TyDi QA, Hotpot QA, and Musique, using instruction-tuned LLMs in different scales demonstrate superior accuracy and significant computational efficiency improvements compared to the previous baselines. Furthermore, our mechanistic analysis reveals specific attention heads and multilayer perceptron (MLP) layers responsible for context attribution, providing valuable insights into the internal workings of RAG models and how they affect RAG behaviours. Code is available at https://github.com/ruizheliUOA/ARC_JSD.

1 Introduction

Retrieval-Augmented Generation (RAG), leveraging large language models (LLMs), has demonstrated significant potential in both academic research [26, 43, 28] and industrial applications [39, 14] by enhancing the accuracy and grounding of generated responses through external contexts such as provided documents or retrieved articles online. A key benefit of RAG lies in its ability to mitigate the hallucination by explicitly attributing generated responses to specific segments of the provided context, known as *context attribution*² [33, 25, 6, 3].

Nevertheless, verifying the extent to which generated responses are genuinely grounded in their cited context remains a challenging task. Current approaches frequently rely heavily on human annotation [23, 27] or computationally expensive methods such as model fine-tuning and gradient-based feature attribution for accurate attribution [42, 25, 3], particularly when dealing with extensive documents. For instance, [25] utilised distribution shifts between responses generated with and without context to identify relevant tokens and employed gradient-based feature attribution to pinpoint context relevance. Similarly, [3] enhanced context attribution accuracy through reward-driven fine-

* Corresponding Author: ruizhe.li@abdn.ac.uk

²We use the term *context attribution* in this work, and there are several different terms used in this area, such as citation, self-citation, etc.

tuning within a Direct Preference Optimisation (DPO) framework, based on probability drop and hold analysis of model outputs to context ablation.

To circumvent these computationally intensive methods, [6] introduced an inference-time attribution mechanism premised on the assumption that if removing grounded context segments substantially reduces the probability of a generated response, those segments are deemed necessary. Conversely, if retaining only grounded segments maintains response probability, these segments are considered sufficient. By capturing hundreds of probability ablation variations per context-response pair, [6] trained a linear surrogate model based on those hundreds of vectors, including the context segment masks and the corresponding generation probability of the original response, to identify context segments crucial for grounding model responses.

However, [6] still need hundreds of RAG model’s forward calls to collect probability ablation samples for the linear surrogate model training. We propose a novel inference-time **Jensen–Shannon Divergence** driven method to **Attribute Response to Context** (ARC-JSD), building upon the inference-attribution assumption above. Our method evaluates the divergence in response distributions generated under the full context compared to sentence-ablated contexts, ranking context sentences based on their JSD differences because of JSD’s symmetric, finite, scale-free, and bounded properties (see § 3 and § 8 for details). This approach offers a significant computational advantage, as it eliminates the need for any additional fine-tuning or surrogate modelling. Furthermore, our ARC-JSD can avoid missing or smoothing non-linearities using JSD to directly quantify actual output distribution shift compared to the linear surrogate modelling [6].

We empirically evaluate our JSD-driven context attribution approach across multiple question-answering benchmarks, i.e., TyDi QA [4], Hotpot QA [40], and MuSiQue [31], using state-of-the-art instruction-tuned LLMs including Qwen2-1.5B-Instruct, Qwen2-7B-Instruct [39], Gemma2-2B-Instruct, and Gemma2-9B-Instruct [30]. Our results not only demonstrate improved average accuracy over 10% in context attribution but also achieve computational efficiency, achieving up to a three-fold speedup compared to [6]’s linear-surrogate-based and other gradient-based baselines.

Moreover, we investigate deeper into a mechanistic exploration of context attribution within RAGs by integrating JSD-based analysis with Logit Lens [24]. Through systematic probing, we identify specific attention heads and MLP layers critical for context attribution. By subsequently manipulating these located attention heads and MLPs using JSD scores as confidence gates, we can control RAGs and further mitigate the hallucination rate. In addition, we can visualise how relevant knowledge is stored in the corresponding MLP layers.

In summary, our primary contributions include:

1. Developing a JSD-driven context attribution method that accurately identifies context critical for grounding responses without requiring fine-tuning, surrogate modelling or gradient calculation.
2. Proposing a computationally efficient solution that can be readily integrated into any existing RAGs. Conducting a detailed mechanistic analysis of RAG, systematically uncovering and validating attention heads and MLP layers responsible for context attribution behaviours.
3. Mitigating the hallucination rate and controlling RAG behaviour by manipulating located attention heads and MLPs within RAG.

2 Related Work

Context attribution for RAG. Prior works for context attribution mainly focus on teaching RAG LLMs to generate self-citations for responses, such as few-shot in-context learning [11], instruction fine-tuning [41]. Some post-hoc works [2, 25] used an auxiliary language model or gradient-based feature attribution to locate relevant context segments. In general, those methods for context attribution are *corroborative* [36] in nature, as citations within context are evaluated on whether they *support* or *imply* a generated response. Meanwhile, [6, 3, 5, 19] including our work focus on the *contributive* attribution methods, which are used to identify whether citations *cause* RAG LLMs to generate a response. [3] proposed a reward-based fine-tuning with DPO to guide RAG LLMs for context attribution, and [6, 5] further trained a linear surrogate model to identify context segments crucial for grounding model responses. [19] focuses on formalising and comparing different attribution acceleration methods and ignores attribution accuracy improvements. However, compared to [6, 3, 5]

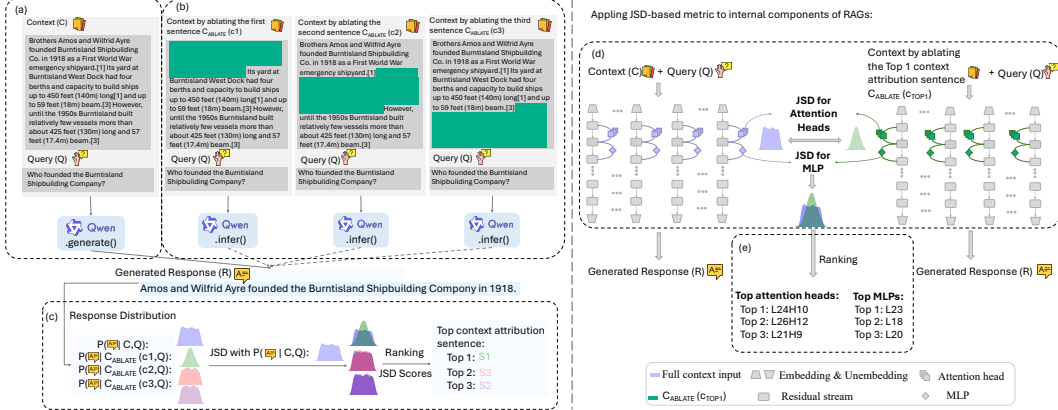


Figure 1: This framework demonstrates how our ARC-JSD works: (a) a RAG LLM $P_{LM}(\cdot)$ first generates response \mathcal{R} conditioned on full context \mathcal{C} and query Q input; (b) By ablating single context sentence once a time, we can calculate probability distribution of the same response \mathcal{R} conditioned on the ablated context $\mathcal{C}_{ABLADE}(c_i)$ and query Q ; (c) We further calculate JSD scores about probability distribution of the same response \mathcal{R} conditioned on full context and ablated context, and locate the most relevant context sentence supporting \mathcal{R} with the highest JSD score. Then, we apply JSD-based metric to internal components of RAGs: (d) For each attention head or MLP output at each layer, we calculate probability distribution of the same response \mathcal{R} conditioned on the same query Q with full context \mathcal{C} and ablated context $\mathcal{C}_{ABLADE}(c_{top-1})$ by removing top relevant context sentence based on § 4.1; (e) We can further locate top- N relevant attention heads or MLPs which contribute the context attribution by ranking the collected JSD scores with a descending order.

and corroborative methods above, our ARC-JSD method eliminates the need for any additional fine-tuning or surrogate modelling, and it can be directly integrated into any existing RAGs.

Mechanistic analysis for RAG. Existing mechanistic studies focus on next token generation task to analyse internal mechanisms of attention heads or MLPs, such as hallucination detection [10], multiple-choice questions [18, 35, 34] and knowledge editing [20, 22, 17]. Recently, [29] used a mechanistic interpretability method to analyse attention heads and MLPs of RAGs for the hallucination detection task. Compared to [29] focusing on locating sources which leads to hallucinations, our proposed ARC-JSD can be regarded as a complementary method to locate citations within context segments and analyse attentions and MLPs, which *causes* RAG LLMs to generate a correct response. [37] focuses on mechanistically analysing retrieval attention heads of RAG LLMs under the Needle-in-the-Haystack (NIAH) setting, where they mainly evaluate whether retrieval attention heads conduct a copy-and-paste operation for retrieving a semantically irrelevant “needle” sentence from the context to the model’s outputs. Compared to [37], which restricts their mechanistic analysis to the NIAH setting where the model performs copy-and-paste retrieval, our work investigates how RAG LLMs mechanistically generate responses based on retrieved content through paraphrasing and contextual integration. This setting better reflects real-world RAG applications³, where models rarely copy text exactly but instead synthesise and rephrase information from retrieved sources.

3 Background

Problem Setup. Consider an autoregressive Transformer-based language model (LLM), denoted as $P_{LM}(\cdot)$. Under RAG settings, this model generates responses (\mathcal{R}) based on an input query (Q) and associated context (\mathcal{C}). Formally, response generation process can be described as $\mathcal{R} \sim P_{LM}(\cdot|\mathcal{C}, Q)$, where context \mathcal{C} consists of sentences $(c_1, c_2, \dots, c_{|\mathcal{C}|})$, the query Q comprises tokens $(q_1, q_2, \dots, q_{|Q|})$, and the generated response \mathcal{R} includes tokens $(r_1, r_2, \dots, r_{|\mathcal{R}|})$. Our analysis of context attribution focuses on how the entire response distribution changes when conditioned

³Compared to traditional RAG to directly map prompts based on their word embeddings, our work has a more general setting, which avoids potential embedding mismatch due to the common paraphrase of RAGs.

on the full context set and ablated context alongside the query: $\mathcal{R} \sim \mathcal{P}_{\text{LM}}(\cdot | c_1, \dots, c_{|\mathcal{C}|}, \mathcal{Q})$, $\mathcal{R} \sim \mathcal{P}_{\text{LM}}(\cdot | \mathcal{C}_{\text{ABLATE}}(c_i), \mathcal{Q})$ where $\mathcal{C}_{\text{ABLATE}}(c_i) = \mathcal{C} \setminus \{c_i\}$, $i \in \{1, \dots, |\mathcal{C}|\}$.

Logit Lens. Logit lens [24] is a mechanistic interpretability method designed to analyse intermediate representations within autoregressive Transformers. Given the LLM architecture described in Appendix D, logit lens leverages intermediate representations to quantify the direct contribution of attention heads ($\mathbf{a}_i^{\ell,h}$), MLP outputs (\mathbf{m}_i^{ℓ}), and residual streams (\mathbf{x}_i^{ℓ}) to token logits: $\text{logit}_i^{\ell,h}(\mathbf{a}_i^{\ell,h}) = W_U \sigma(\mathbf{a}_i^{\ell,h})$, $\text{logit}_i^{\ell}(\mathbf{m}_i^{\ell}) = W_U \sigma(\mathbf{m}_i^{\ell})$, $\text{logit}_i^{\ell}(\mathbf{x}_i^{\ell}) = W_U \sigma(\mathbf{x}_i^{\ell})$. Thus, logit lens serves as a powerful tool for pinpointing specific model components crucial to prediction behaviours.

JSD for Context Attribution. JSD is a symmetrised, smoothed variant of Kullback–Leibler (KL) divergence that quantifies information gap (in bits) between two probability distributions. Because it is symmetric, finite, scale-free, and bounded in $[0, \log 2]$, JSD allows scores from different layers to be compared directly, without sensitivity to arbitrary logit shifts. Following “logit-lens” perspective of [29], we treat JSD as model’s belief of how much its next-token distribution will change. Concretely, we compute JSD between the full-context token distribution and the distribution obtained after removing a single retrieved sentence c_i . A high divergence indicates that the model’s internal representations (and therefore its output logits) depend strongly on c_i . Empirically, ablating the sentence with the highest JSD causes the largest drop in answer likelihood, validating JSD as a concise and reliable signal for context attribution in RAG models (See § 8 for comparisons among JSD, Wasserstein, Total Variation (TV) and Maximum Mean Discrepancy (MMD)).

4 Attributing Top Relevant Context Sentences via JSD

4.1 Identifying Relevant Context via JSD

Following assumption proposed by [6], removal of context segments critical to generating a specific response \mathcal{R} significantly impacts probability distribution of that response. Conversely, the removal of less relevant context segments is expected to minimally affect probability distribution of \mathcal{R} .

Unlike the approach by [6], which requires extensive sampling of ablated contexts for each $(\mathcal{C}, \mathcal{Q})$ pair and training a surrogate model to learn context-response relationships, our proposed ARC-JSD method relies purely on inference in the Fig. 1. Specifically, we compute the JSD between the response probability distributions conditioned on the full context \mathcal{C} and on each context-ablated variant $\mathcal{C}_{\text{ABLATE}}(c_i)$:

$$\text{JSD}(c_i) = \sum_{j=1}^{|\mathcal{R}|} \text{JSD}(\mathcal{P}_{\text{LM}}(r_j | \mathcal{C}, \mathcal{Q}) || \mathcal{P}_{\text{LM}}(r_j | \mathcal{C}_{\text{ABLATE}}(c_i), \mathcal{Q})) \quad (1)$$

where we use $\text{JSD}(c_i)$ to aggregate the JSD score of each generated tokens r_j from \mathcal{R} when the context sentence c_i is ablated from the context \mathcal{C} . By calculating JSD scores for all sentences in the context, we identify the most relevant context sentence c_i by selecting the sentence based on the assumption about the significant impact of removing critical context segments: $c_{\text{Top-1}} = \arg \max_{c_i \in \mathcal{C}} (\{\text{JSD}(c_i)\}_{i=1}^{|\mathcal{C}|})$.

4.2 Evaluation of Context Attribution Accuracy

To assess efficacy of our ARC-JSD method, we conduct experiments on three widely recognised question-answering datasets commonly used in RAG studies: *TyDi QA* [4]: a multilingual QA dataset using entire Wikipedia articles as external context (we only use English part), *Hotpot QA* [40]: a multi-hop QA dataset requiring reasoning for questions based on multiple documents, and *MuSiQue* [31]: a high-quality multi-hop QA benchmark over Wikipedia

Table 1: The FLOPs for each baseline and ARC-JSD, where P indicates the number of target model parameters, T indicates the number of tokens per context sentence, L is layer numbers of target model, $|\mathcal{R}|$ and $|\mathcal{C}|$ indicates the number of response tokens and context sentences, respectively.

Baselines	Theoretical FLOPs	Slowdown over ARC-JSD
ALTI-Logit	$2PT \mathcal{C} \mathcal{R} L$	$ \mathcal{R} L/ \mathcal{C} $
MIRAGE	$4PT \mathcal{C} (2 \mathcal{C} + 1)$	$4 + 2/ \mathcal{C} $
Contextcite (32 calls)	$2PT \times 32^2$	$(32/ \mathcal{C})^2$
Contextcite (256 calls)	$2PT \times 256^2$	$(256/ \mathcal{C})^2$
ARC-JSD (key-value caching)	$2PT \mathcal{C} ^2$	1

that highlights minimal context and multiple valid reasoning paths to evaluate complex reasoning capabilities. Moreover, we evaluate our ARC-JSD with different training-free baselines for context attribution: *ALTI-Logit* [9]: a method to directly compare logit difference between input context and generation on token level by accumulating layerwise logit; *MIRAGE* [25]: a gradient-based and token-level method to locate context-sensitive tokens using contrastive feature attribution; *Contextcite* [6]: a post-hoc method to train a linear surrogate model based on a fixed group of context ablation forward runs. Table 2 summarises the statistics of these datasets, where *MuSiQue* has the longest context input compared to others with the average length of context in sentences $|\mathcal{C}| = 93.6$. Our evaluations involve four instruction-tuned LLMs of varying scales, namely Qwen2-1.5B-IT, Qwen2-7B-IT [39], Gemma2-2B-IT, and Gemma2-9B-IT [30]. For each dataset, we randomly select up to 1,000 samples from their development sets. All models are evaluated in inference mode without further fine-tuning. We mainly evaluate the top-1 context attribution accuracy, which indicates the percentage of overlap between the predicted top-1 context sentence and gold-standard sentence on the datasets⁴. For ALTI-Logit and MIRAGE, which mainly focus on token-level attribution, we use the accumulated operations to locate sentence-level context attribution prediction (Appendix E includes more details).

Table 1 lists theoretical floating-point operations (FLOPs) for each method, where we follow the assumption from [16, 15], i.e., one forward pass needs approximately $2PT$ FLOPs. ARC-JSD is considerably cheaper than baselines because it pinpoints salient context sentences without back-propagation or iterative token masking. ContextCite requires a fixed 32 or 256 forward passes; this is economical only when input contains more than 32 or far more than 256 sentences, respectively, but its context attribution accuracy remains below that of ARC-JSD (see Fig. 2(a)). Fig. 2(a) presents compute-accuracy trade-off on MuSiQue dataset across all baselines and LLM backbones. It clearly demonstrates that ARC-JSD consistently outperforms all baselines, yielding an average context attribution accuracy improvement of approximately 10.7%. Although Contextcite-32 is more efficient when $|\mathcal{C}|$ is larger than 32, its attribution accuracy lags behind ARC-JSD. Overall, our method offers substantial computational efficiency improvements, achieving up to 3-fold speedups and consistently align with Pareto-optimal over multiple orders of magnitude for different LLM backbones. In addition, we utilise GPT-4.1 mini as a judge to compare whether generated responses of all RAG models are semantically equivalent to the corresponding gold answers from datasets when context attribution is correct. The average accuracy is up to 99.3% (See Appendix G and F for details).

5 Mechanistically Study RAG LLMs for Context Attribution

5.1 Locating Relevant Attention Heads and MLPs

To better understand internal mechanisms by which RAG LLMs attribute generated responses to their relevant context sentences, we systematically investigate specific attention heads and MLP layers involved. Our method combines the ARC-JSD metric described previously (§ 4.1) with the Logit Lens [24] to precisely quantify contributions from these internal model components.

Following the ARC-JSD framework in the § 4.1, we apply JSD difference at the level of individual attention heads and MLP layers, comparing their outputs between scenarios involving full context

Table 2: The size of three benchmarks randomly sampled from their development dataset is up to 1000, where the average word numbers and sentence numbers of context (i.e., $|\mathcal{C}|$) are summarised.

Datasets	Size	Contexts	
		Avg. Words	Avg. Sents.
TyDi QA	440	99.5	4.8
Hotpot QA	1,000	940.3	51.1
MuSiQue	1,000	1753.8	93.6

⁴We choose sentence level because current QA datasets only have sentence-level gold labels to evaluate attribution accuracy. However, our ARC-JSD method can be extended to finer-grained interactions such as phrases or sub-sentences spans by dynamically selecting the start and end token indices.

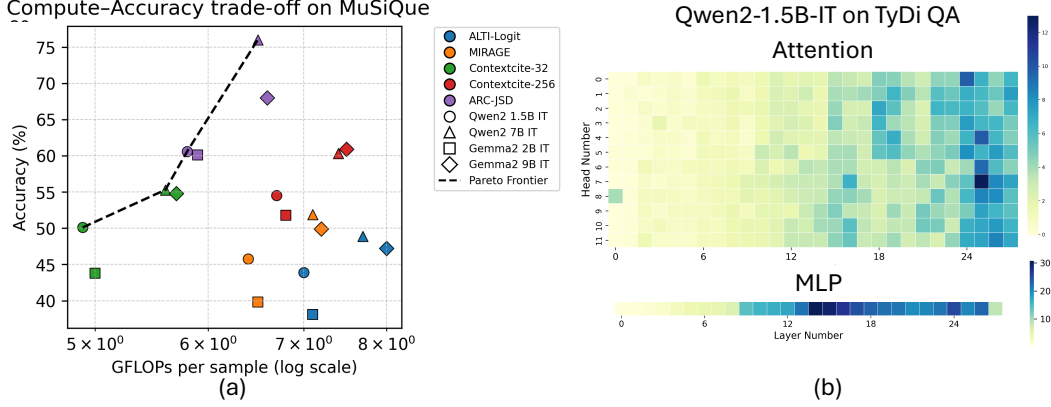


Figure 2: (a) The compute-accuracy trade-off on MuSiQue for 4 baselines and ARC-JSD on 4 LLM backbones with GFLOPs \log_{10} scale per sample; (b) The average JSD score of attention heads and MLP of Qwen2-1.5B-IT on TyDi QA across all layers. The deeper colour indicates larger JSD scores.

and the ablation of the most relevant context sentence using Eq. 1:

$$\begin{aligned} \text{JSD}_{\text{Attn}}^{\ell, h} &= \sum_{j=1}^{|\mathcal{R}|} \text{JSD} \left(\mathcal{P}_{\text{Attn}}^{\ell, h}(r_j | \mathcal{C}, \mathcal{Q}) || \mathcal{P}_{\text{Attn}}^{\ell, h}(r_j | \mathcal{C}_{\text{ABLATE}}(c_{\text{top-1}}), \mathcal{Q}) \right) \\ \text{JSD}_{\text{MLP}}^{\ell} &= \sum_{j=1}^{|\mathcal{R}|} \text{JSD} \left(\mathcal{P}_{\text{MLP}}^{\ell}(r_j | \mathcal{C}, \mathcal{Q}) || \mathcal{P}_{\text{MLP}}^{\ell}(r_j | \mathcal{C}_{\text{ABLATE}}(c_{\text{top-1}}), \mathcal{Q}) \right) \end{aligned} \quad (2)$$

where $\mathcal{P}_{\text{Attn}}^{\ell, h}()$ and $\mathcal{P}_{\text{MLP}}^{\ell}()$ denote the probability distributions derived from attention head outputs $\mathbf{a}_j^{\ell, h}$ and MLP outputs \mathbf{m}_j^{ℓ} , respectively, via the logit lens and softmax operations:

$$\mathcal{P}_{\text{Attn}}^{\ell, h}() = \text{Softmax}(\text{logit}(\mathbf{a}_j^{\ell, h})), \quad \mathcal{P}_{\text{MLP}}^{\ell}() = \text{Softmax}(\text{logit}(\mathbf{m}_j^{\ell})) \quad (3)$$

where the shape of attention head output $\mathbf{a}^{\ell, h}$ and MLP output \mathbf{m}^{ℓ} is $[1, d]$, and d is dimensionality of residual stream. By computing JSD scores across all heads and MLP layers, we rank these components according to their relevance to context attribution:

$$J_{\text{Top-}N}(\text{Attn}) = \text{sort} \left(\{\text{JSD}_{\text{Attn}}^{\ell, h}\}_{\ell=0, h=0}^{L, H}, \text{descending} \right), \quad J_{\text{Top-}N}(\text{MLP}) = \text{sort} \left(\{\text{JSD}_{\text{MLP}}^{\ell}\}_{\ell=0}^L, \text{descending} \right) \quad (4)$$

5.2 Mechanistic Insights from Located Attention Heads and MLPs

Applying the methodology described in § 5.1, we conducted experiments across three benchmark datasets (see § 4.2) using various LLM scales. Fig. 2(b) presents the distribution and JSD scores of attention heads identified as most relevant for context attribution in Qwen2-1.5B-Instruct on TyDi QA dataset. Our analysis reveals that the top attention heads contributing to context attribution predominantly reside in the higher layers. This observation holds across most datasets, partially corroborating earlier findings by [37], which indicated that retrieval-related attention heads are typically found in the intermediate and higher layers. Notably, our work expands upon NIAH setting explored by [37] by mechanistically evaluating attention heads and MLPs relevance through paraphrasing and contextual integration of RAG LLMs. This setting better reflects real-world RAG applications, where models rarely copy text exactly but instead synthesise and rephrase information from retrieved sources. Additional visualisations and distributions for another Qwen2-7B-IT and Gemma2 models across all datasets are provided in Appendix I. Similarly, Fig. 2(b) illustrates that intermediate and higher MLP layers also significantly contribute to context attribution. This pattern remains consistent across different datasets and model scales within the same LLM family. Corresponding detailed findings for Qwen2-7B-IT and Gemma2 models are available in Appendix I.

Table 3: Spearman’s ρ of the overlap about top-10 located attentions and MLPs between JSD-based mechanistic and semantic gain-based metrics over all datasets and RAG models. \diamond and \blacklozenge indicate p -value is < 0.05 and < 0.01 , respectively.

Modules	Top-10	Datasets	Qwen2 1.5B IT		Qwen2 7B IT		Gemma2 2B IT		Gemma2 9B IT	
			$J(\cdot) \cap S^{(+)}$	$G(\cdot) \cap S^{(+)}$						
Attention	TyDi QA	6.83 \diamond	7.26 \diamond	6.91 \diamond	7.31 \diamond	7.62 \blacklozenge	7.25 \diamond	7.63 \blacklozenge	7.28 \diamond	7.28 \diamond
	Hotpot QA	6.73 \diamond	6.65 \diamond	6.81 \diamond	6.79 \diamond	6.68 \diamond	6.67 \diamond	6.72 \diamond	6.73 \diamond	6.73 \diamond
	MuSiQue	6.67 \diamond	6.72 \diamond	6.72 \diamond	6.83 \diamond	6.69 \diamond	6.71 \diamond	6.73 \diamond	6.75 \diamond	6.75 \diamond
MLP	TyDi QA	6.90 \diamond	7.72 \blacklozenge	6.96 \diamond	7.67 \blacklozenge	7.75 \blacklozenge	8.03 \blacklozenge	7.78 \blacklozenge	8.05 \blacklozenge	8.05 \blacklozenge
	Hotpot QA	6.83 \diamond	7.49 \blacklozenge	6.87 \diamond	7.52 \blacklozenge	7.50 \blacklozenge	8.02 \blacklozenge	7.53 \blacklozenge	8.06 \blacklozenge	8.06 \blacklozenge
	MuSiQue	6.87 \diamond	7.12 \diamond	6.91 \diamond	7.18 \diamond	7.51 \blacklozenge	8.04 \blacklozenge	7.54 \blacklozenge	8.05 \blacklozenge	8.05 \blacklozenge

6 Verification of JSD-based Mechanistic Study

Having identified critical RAG components using JSD in § 5.1, we now seek to verify these findings from a different analytical angle. Our JSD approach measures a component’s dependence on context through ablation. As a crucial cross-check, we introduce the semantic gain metric, which measures a component’s direct contribution to the correct answer when the full context is present. This allows us to test a key hypothesis: components that are truly important for attribution should not only depend on the context (high JSD) but also actively use it to improve the answer (high semantic gain). Demonstrating a strong correlation between these metrics will robustly verify that the components we located are indeed the primary drivers of context attribution.

6.1 Semantic Gains of Attention and MLPs for Context Attribution

Apart from locating relevant attention heads and MLPs using JSD-based metric from the § 5.1, we also know that semantic information of context attribution from attentions and MLPs will be added back to the residual stream from each layer based on the autoregressive language model’s architecture from the § 3 [8, 17]. Based on such properties, we can verify whether the JSD-based metric for attention and MLPs location in the § 5.1 works by projecting the residual stream before and after each layer’s attention and MLPs components into the vocabulary space, and calculating the cosine similarity with the generated response \mathcal{R} to further identify which attention and MLP modules provide higher semantic gains.

Based on the introduction of internal mechanism of LLMs in the § 3 and full context \mathcal{C} with query \mathcal{Q} as model’s input, we further split the residual stream flow of each layer into three parts for each generated token t_i , i.e., pre-residual stream $\mathbf{x}_i^{\ell,\text{pre}}$, middle-residual stream $\mathbf{x}_i^{\ell,\text{mid}}$ and post-residual stream $\mathbf{x}_i^{\ell,\text{post}}$: $\mathbf{x}_i^{\ell,\text{pre}} = \mathbf{x}_{i-1}^{\ell-1,\text{post}}$, $\mathbf{x}_i^{\ell,\text{mid}} = \mathbf{x}_i^{\ell,\text{pre}} + \mathbf{a}_i^\ell$, $\mathbf{x}_i^{\ell,\text{post}} = \mathbf{x}_i^{\ell,\text{mid}} + \mathbf{m}_i^\ell = \mathbf{x}_i^{\ell+1,\text{pre}}$. After applying the logit lens to $\mathbf{x}_i^{\ell,\text{pre}}$, $\mathbf{x}_i^{\ell,\text{mid}}$ and $\mathbf{x}_i^{\ell,\text{post}}$ via the softmax, we will have the probability distribution of the generated token $t_i^{\ell,\text{pre}}$, $t_i^{\ell,\text{mid}}$ and $t_i^{\ell,\text{post}}$ for each layer, and then we will use greedy decoding to select the top-1 token with the highest probability: $t_i^{\ell,\text{pre/mid/post}} = \arg \max_{t_i^{\ell,\text{pre/mid/post}} \in \mathcal{V}} (\text{softmax}(\text{logit}(\mathbf{x}_i^{\ell,\text{pre/mid/post}})))$.

Consequently, we can project the selected token $t_i^{\ell,\text{pre/mid/post}}$ into the vocabulary embedding space via the unembedding matrix $W_U \in \mathbb{R}^{d \times |\mathcal{V}|}$: $\mathbf{e}_i^{\ell,\text{pre/mid/post}} = W_U[:, t_i^{\ell,\text{pre/mid/post}}]$. We can calculate the corresponding semantic gains $\Delta_i^{\ell,\text{Attn}}$ and $\Delta_i^{\ell,\text{MLP}}$ via attention and MLP modules using the cosine similarity difference with the generated response token embedding $\mathbf{e}_i = W_U[:, r_i]$: $\Delta_i^{\ell,\text{Attn}} = \cos(\mathbf{e}_i^{\ell,\text{mid}}, \mathbf{e}_i) - \cos(\mathbf{e}_i^{\ell,\text{pre}}, \mathbf{e}_i)$, $\Delta_i^{\ell,\text{MLP}} = \cos(\mathbf{e}_i^{\ell,\text{post}}, \mathbf{e}_i) - \cos(\mathbf{e}_i^{\ell,\text{mid}}, \mathbf{e}_i)$. Finally, we will average across the entire generated responses \mathcal{R} and calculate the semantic gains $\Delta^{\ell,\text{Attn}}$ and $\Delta^{\ell,\text{MLP}}$ for attention MLP of each layer, and collect and sort the semantic gains of attention and MLP from all layer with descending order:

$$\Delta^{\ell,\text{Attn}} = \frac{1}{|\mathcal{R}|} \sum_i^{\mathcal{R}} \Delta_i^{\ell,\text{Attn}}, \quad \Delta^{\ell,\text{MLP}} = \frac{1}{|\mathcal{R}|} \sum_i^{\mathcal{R}} \Delta_i^{\ell,\text{MLP}} \quad (5)$$

$$G_{\text{Top-}N}(\text{Attn}) = \text{sort}(\{\Delta^{\ell,\text{Attn}}\}_{\ell=0}^L, \text{descending}), \quad G_{\text{Top-}N}(\text{MLP}) = \text{sort}(\{\Delta^{\ell,\text{MLP}}\}_{\ell=0}^L, \text{descending}) \quad (6)$$

6.2 Mutually Verifying JSD-based Mechanistic Study via the Semantic Gains of Attention and MLPs

Based on the Eq. 4 and Eq. 6, we can locate layer-wise attention and MLP components relevant to context attribution from two different perspectives in the § 5.1 and § 6.1. We can evaluate the correlation of both metrics and further verify the effectiveness of our proposed ARC-JSD metric in the § 4.1 and § 5.1.

Given $\{\text{JSD}_{\text{MLP}}^{\ell}\}_{\ell=0}^L$ and $\{\Delta^{\ell, \text{MLP}}\}_{\ell=0}^L$ via the JSD-based and Semantic-gain-based metrics, we first define an average-ranking fusion, called *consensus* $S^{(+)}$, to fuse both JSD and semantic gain views, which is based on the assumption that a layer is important if both metrics sort the layer highly:

$$S^{(+)} = \frac{1}{2} (\text{ranking}_J + \text{ranking}_G) = \frac{1}{2} \left(\frac{\text{ranking of } (\{\text{JSD}_{\text{MLP}}^{\ell}\}_{\ell=0}^L)}{L} + \frac{\text{ranking of } (\{\Delta^{\ell, \text{MLP}}\}_{\ell=0}^L)}{L} \right) \quad (7)$$

where ranking of (\cdot) will assign 1 to the largest $\text{JSD}_{\text{MLP}}^{\ell}$ or $\Delta^{\ell, \text{MLP}}$ and the smallest $\text{JSD}_{\text{MLP}}^{\ell}$ or $\Delta^{\ell, \text{MLP}}$ will be assigned L . Then we uniform and remove the layer influence divided by L to get ranking_J and ranking_G , whose range is $[1/n, 1]$, i.e., a smaller fraction will have a higher ranking ($1/n$ is best). Finally, we take the average of the ranking_J and ranking_G as the *consensus* $S^{(+)}$, where a smaller consensus inside of $S^{(+)}$ will indicate a stronger joint evidence that both metrics consider the layer important, and a larger consensus means at least one metric puts the layer far down the list. Finally, we calculate Spearman ρ of $J_{\text{Top}-N}(\text{MLP}) \cap S_{\text{Top}-N}^{(+)}$ and $G_{\text{Top}-N}(\text{MLP}) \cap S_{\text{Top}-N}^{(+)}$, where $S_{\text{Top}-N}^{(+)} = \text{sort}(S^{(+)}, \text{ascending})$. For attention components, we first average JSD scores of all attention heads in the same layer to build $\{\text{JSD}_{\text{Attn}}^{\ell}\}_{\ell=0}^L = \{\frac{1}{H} \sum_{h=0}^H \text{JSD}_{\text{Attn}}^{\ell, h}\}_{\ell=0}^L$, and then further calculate ρ of $J_{\text{Top}-N}(\text{Attn}) \cap S_{\text{Top}-N}^{(+)}$ and $G_{\text{Top}-N}(\text{Attn}) \cap S_{\text{Top}-N}^{(+)}$. The benefit of using *consensus* $S^{(+)}$ instead of the raw JSD or semantic gain values is that $S^{(+)}$ will remove all scaling issue due to the different units and variances of JSD or semantic gains, and a single extremely large JSD or semantic gain will not swamp the fusion, which is robust to outliers.

Table 3 reports significant Spearman ρ values for overlap between top-10 attention/MLP layers ranked by JSD and by semantic gain. This frequent co-occurrence indicates that both metrics track the same retrieval-driven signal that improves next-token prediction. Intuitively, when a layer genuinely draws on a retrieved sentence c_i to write answer, ablating c_i (i) alters that layer’s token distribution yielding high JSD and (ii) removes the “helpful push” toward the correct token lowering semantic gain. Layers that merely supply generic syntax or parametric knowledge may boost semantic gain without changing under ablation, so their JSD remains low; the strong overall correlation shows that such cases do not dominate, which further verifies effectiveness of ARC-JSD. In addition, ARC-JSD is practical: it requires only forward passes, avoiding cost and saturation issues of gradient-based saliency [25]. Unlike KL (undefined with zero-probability bins) or logit-space ℓ_2 distances (scale-dependent) [9], JSD is finite, symmetric, scale-free, and measured in interpretable bits.

7 Case Studies of Located Attention Heads and MLPs

Visualisation of MLPs. Based on semantic gains analysis from § 6.2, we visualise projection of middle-residual stream $\mathbf{x}_i^{\ell, \text{mid}}$ and post-residual stream $\mathbf{x}_i^{\ell, \text{post}}$ via Logit Lens to vocabulary space in Fig. 3 and Appendix K. In Fig. 3, Qwen2-1.5B-IT was given data from TyDi QA dev dataset with context about mosquitos introduction from Wikipedia and query “*How many wings does a mosquito have?*” as input, and it generates responses “*A mosquito has two wings.*” as output. Based on our ARC-JSD method, we successfully located top-relevant context sentence, i.e., “*Mosquitoes have a slender segmented body, a pair of wings, three pairs of long hair-like legs, feathery antennae, and elongated mouthparts*”. When we compare heatmap between $\mathbf{x}_i^{\ell, \text{post}}$ and $\mathbf{x}_i^{\ell, \text{mid}}$ in Fig. 3 from Layer 20 to Layer 27 (See Appendix K for full heatmap), we find that probability of correct token is increased significantly after $\mathbf{x}_i^{\ell, \text{post}}$ compared to $\mathbf{x}_i^{\ell, \text{mid}}$, such as ‘wings’ in Layer 23, ‘A’, ‘has’, ‘two’ in Layer 26, and ‘mosquito’, ‘two’, ‘A’ in Layer 27, which aligns with our findings that MLP contribute more parametric knowledge for context attribution in higher layers using JSD-based metric from § 5.2. Moreover, we find that several correct tokens are gradually transferred from their Chinese format to English version in Qwen2, such as ‘一只 (A)’, ‘拥有 (has)’ and ‘翅膀 (wings)’, which is reasonable

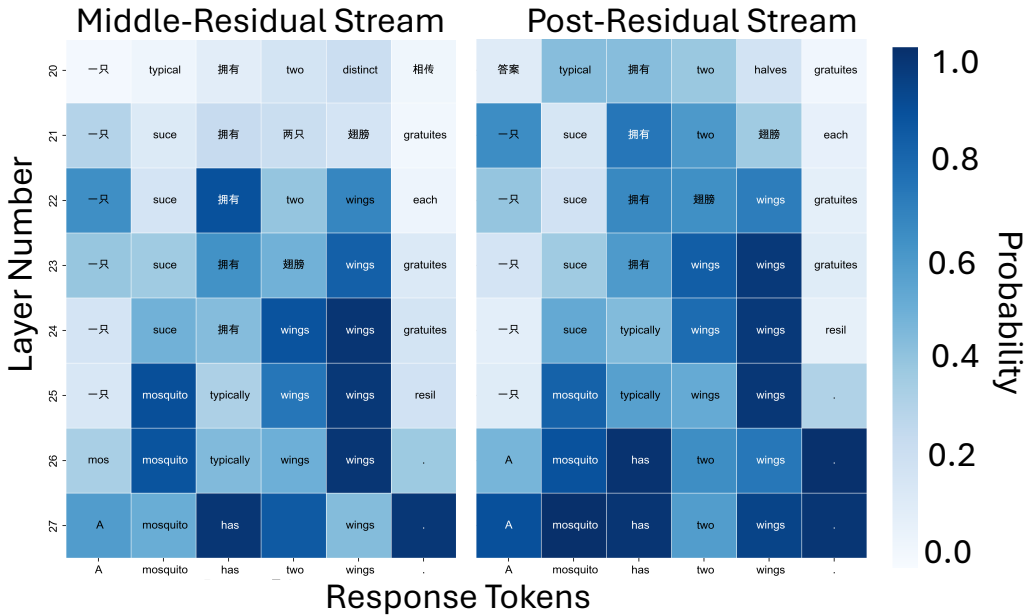


Figure 3: The projection of $\mathbf{x}_i^{\ell, \text{mid}}$ and $\mathbf{x}_i^{\ell, \text{post}}$ via Logit Lens to vocabulary space from layer 20 to layer 27 of Qwen2-1.5B IT in TyDi QA data sample, where the generated response \mathcal{R} is “A mosquito has two wings.” (See Appendix K for all layer projections). Each cell shows the most probable token decoded via Logit Lens. The colour indicates the probability of the decoded token of the corresponding $\mathbf{x}_i^{\ell, \text{mid}}$ or $\mathbf{x}_i^{\ell, \text{post}}$.

Table 4: Hallucination rate and factual information maintenance by gating top-5 JSD-based attention heads and MLP using Qwen2 7B IT on Hotpot QA dataset. \dagger : Hallucination = RAG-generated response contradicts ground-truth while attributed context contained that ground-truth. \ddagger : we use JSD scores as a confidence gate to top-relevant attention heads and MLP layers with Mask = $0.7 + 0.3 \times \text{sigmoid}(G)$, which means that top-relevant JSD attention and MLP will be multiplied with a mask close to 0.7 when their corresponding semantic gain G is smaller than 0.

Setup for Qwen2 7B IT	Hallucination Rate †	Pass@1 Factual F1	Notes
Base RAG	13.4%	76.1	One retrieved context sentence contains the answer
Gate Top-5 Attn & MLP ‡	8.2%	75.9	Mask is 0.7 on top-5 JSD Attn & MLP when their $G < 0$
Gate Random 5 Attn & MLP	12.7%	69.4	Control

as Chinese is one of main language resources used in Qwen2 pre- and post-training [39]. This finding also matches observations [38] that representations tend to be anchored by semantically-equivalent dominant-language tokens in higher layers.

Control RAGs based on ARC-JSD located Attention & MLPs. Moreover, we conduct an ablation study to compare the JSD difference of responses by masking the top-10 relevant attention heads and randomly-selected 10 attention heads in Table 5. Generally, ablating attention heads located by using JSD-based metric causes larger JSD scores compared to the random attention heads ablation, which further verifies our proposed ARC-JSD can identify context-attribution-related attention heads. To further evaluate how the located internal components affect RAG behaviours, we conduct extra experiments on Qwen2 7B IT to demonstrate whether ARC-JSD can reduce hallucinations and maintain factual information at the same time. We select 200 data samples from Hotpot QA where Qwen2 7B IT did not provide a truthful response compared to the ground truth. From Table 4, we can use the JSD attribution

Table 5: Comparison of average JSD scores between masking top-10 relevant attention heads and randomly masking 10 attention heads using all RAG models on all datasets.

Top-10 Attention Heads	Random 10 Attention Heads
2.23 ± 0.12	1.53 ± 0.76

scores and semantic gain G as a confidence gate to reduce the hallucination rate by $\approx 39\%$ without hurting factual F1 compared to random gating attention and MLPs.⁵.

8 Discussion

Comparison JSD with KL, Wasserstein, TV and MMD. In Fig. 4, we conduct an ablation study among different metrics, which shows that JSD works better than other metrics regarding compute-accuracy trade-off. Here, we discuss some possible reasons: *KL divergence* will explode whenever ablated run assigns ≈ 0 probability to a token when full run uses (it is common in deep layers of LLMs). The unbounded scale makes it impossible to compare “how much layer 7 changed” to “how much layer 28 changed”; *TV* distance is bounded but too coarse, which means that two distributions that swap 5% mass on high-entropy tails give the same TV as two distributions that shift 5% mass off the top-1 token, yet the latter wrecks the answer; *Wasserstein* needs a distance between tokens. There is no canonical ground metric on a 152K vocabulary (Qwen2-7B-Instruct version), and any choice (e.g., edit distance, embedding cosine, etc.) injects an orthogonal modelling assumption and costs $O(V^3)$ per layer; *MMD* always requires a kernel and a feature map to measure a Reproducing kernel Hilbert space (RKHS) norm, which is not tied to likelihood or entropy. It also needs a notion of distance between tokens to build the kernel (See Appendix J for details and examples).

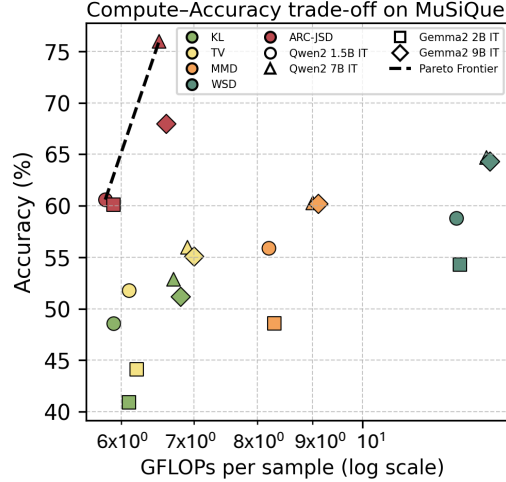


Figure 4: The compute-accuracy trade-off on MuSiQue for different metrics and ARC-JSD on 4 LLM backbones with GFLOPs log₁₀ scale per sample.

What if all JSD scores are very small? When all scores are very small, it is the attribution. Small everywhere is not an error, and it means that RAG answers from parametric memory or retrieved passages are irrelevant. In those cases, we prefer to return “no evidence passage was used” rather than force-label the least-bad one. Practically, we can flag the answer with “low-evidence” when all sentence-JSD < 0.02 bits (\approx median noise). The benefit than a threshold is that we can distinguish “no context used” from “weak but present context” without having to guess a universal cut-off. We could use that signal to re-query or warn the user, which is in practice a more faithful and safer behaviour than picking the least-small score.

9 Conclusion

We introduce ARC-JSD, an inference-time JSD-based metric that directly attributes RAG responses to their source sentences with no fine-tuning or surrogate models needed. Across diverse QA benchmarks and instruction-tuned LLMs, ARC-JSD outperforms different baselines in attribution accuracy while cutting computational overhead; when paired with the Logit Lens, it even pinpoints the specific attention heads and MLPs driving those attributions, advancing the mechanistic interpretability and transparency of RAG systems.

Acknowledgement

This work is supported by the Gemma 2 Academic Program GCP Credit Award from Google.

⁵This experiment mainly evaluates how our ARC-JSD located attention and MLP affect the hallucinations and factual information in the RAG response based on the well-known agreement that attention heads and MLP focus on retrieval behavior and knowledge storage [29], respectively.

References

- [1] S. Bird, E. Klein, and E. Loper. *Natural language processing with Python: analyzing text with the natural language toolkit.* "O'Reilly Media, Inc.", 2009.
- [2] A. Chen, P. Pasupat, S. Singh, H. Lee, and K. Guu. Purr: Efficiently editing language model hallucinations by denoising language model corruptions. *arXiv preprint arXiv:2305.14908*, 2023.
- [3] Y.-S. Chuang, B. Cohen-Wang, S. Z. Shen, Z. Wu, H. Xu, X. V. Lin, J. Glass, S.-W. Li, and W.-t. Yih. Selfcite: Self-supervised alignment for context attribution in large language models. *arXiv preprint arXiv:2502.09604*, 2025.
- [4] J. H. Clark, E. Choi, M. Collins, D. Garrette, T. Kwiatkowski, V. Nikolaev, and J. Palomaki. Tydi qa: A benchmark for information-seeking question answering in typologically diverse languages. *Transactions of the Association for Computational Linguistics*, 8:454–470, 2020.
- [5] B. Cohen-Wang, Y.-S. Chuang, and A. Madry. Learning to attribute with attention. *arXiv preprint arXiv:2504.13752*, 2025.
- [6] B. Cohen-Wang, H. Shah, K. Georgiev, and A. Madry. Contextcite: Attributing model generation to context. *Advances in Neural Information Processing Systems*, 37:95764–95807, 2024.
- [7] D. Dai, L. Dong, Y. Hao, Z. Sui, B. Chang, and F. Wei. Knowledge neurons in pretrained transformers. In *Proceedings of the 60th Annual Meeting of the Association for Computational Linguistics (Volume 1: Long Papers)*, pages 8493–8502, 2022.
- [8] N. Elhage, N. Nanda, C. Olsson, T. Henighan, N. Joseph, B. Mann, A. Askell, Y. Bai, A. Chen, T. Conerly, et al. A mathematical framework for transformer circuits. *Transformer Circuits Thread*, 1:1, 2021.
- [9] J. Ferrando, G. I. Gállego, I. Tsiamas, and M. R. Costa-jussà. Explaining how transformers use context to build predictions. *arXiv preprint arXiv:2305.12535*, 2023.
- [10] J. Ferrando, O. B. Obeso, S. Rajamanoharan, and N. Nanda. Do i know this entity? knowledge awareness and hallucinations in language models. In *The Thirteenth International Conference on Learning Representations*, 2025.
- [11] T. Gao, H. Yen, J. Yu, and D. Chen. Enabling large language models to generate text with citations. In *Proceedings of the 2023 Conference on Empirical Methods in Natural Language Processing*, pages 6465–6488, 2023.
- [12] M. Geva, A. Caciularu, K. Wang, and Y. Goldberg. Transformer feed-forward layers build predictions by promoting concepts in the vocabulary space. In *Proceedings of the 2022 Conference on Empirical Methods in Natural Language Processing*, pages 30–45, 2022.
- [13] M. Geva, R. Schuster, J. Berant, and O. Levy. Transformer feed-forward layers are key-value memories. In *Proceedings of the 2021 Conference on Empirical Methods in Natural Language Processing*, pages 5484–5495, 2021.
- [14] D. Guo, D. Yang, H. Zhang, J. Song, R. Zhang, R. Xu, Q. Zhu, S. Ma, P. Wang, X. Bi, et al. Deepseek-r1: Incentivizing reasoning capability in llms via reinforcement learning. *arXiv preprint arXiv:2501.12948*, 2025.
- [15] J. Hoffmann, S. Borgeaud, A. Mensch, E. Buchatskaya, T. Cai, E. Rutherford, D. d. L. Casas, L. A. Hendricks, J. Welbl, A. Clark, et al. Training compute-optimal large language models. *arXiv preprint arXiv:2203.15556*, 2022.
- [16] J. Kaplan, S. McCandlish, T. Henighan, T. B. Brown, B. Chess, R. Child, S. Gray, A. Radford, J. Wu, and D. Amodei. Scaling laws for neural language models. *arXiv preprint arXiv:2001.08361*, 2020.
- [17] S. Katz, Y. Belinkov, M. Geva, and L. Wolf. Backward lens: Projecting language model gradients into the vocabulary space. In *Proceedings of the 2024 Conference on Empirical Methods in Natural Language Processing*, pages 2390–2422, 2024.

[18] R. Li and Y. Gao. Anchored answers: Unravelling positional bias in gpt-2’s multiple-choice questions. *arXiv preprint arXiv:2405.03205*, 2024.

[19] F. Liu, N. Kandpal, and C. Raffel. Attribot: A bag of tricks for efficiently approximating leave-one-out context attribution. *arXiv preprint arXiv:2411.15102*, 2024.

[20] K. Meng, D. Bau, A. Andonian, and Y. Belinkov. Locating and editing factual associations in gpt. *Advances in neural information processing systems*, 35:17359–17372, 2022.

[21] K. Meng, A. S. Sharma, A. J. Andonian, Y. Belinkov, and D. Bau. Mass-editing memory in a transformer. In *The Eleventh International Conference on Learning Representations*, 2022.

[22] K. Meng, A. S. Sharma, A. J. Andonian, Y. Belinkov, and D. Bau. Mass-editing memory in a transformer. In *The Eleventh International Conference on Learning Representations*, 2023.

[23] J. Menick, M. Trebacz, V. Mikulik, J. Aslanides, F. Song, M. Chadwick, M. Glaese, S. Young, L. Campbell-Gillingham, G. Irving, et al. Teaching language models to support answers with verified quotes. *arXiv preprint arXiv:2203.11147*, 2022.

[24] nostalgicbraist. interpreting gpt: the logit lens, 2020.

[25] J. Qi, G. Sarti, R. Fernández, and A. Bisazza. Model internals-based answer attribution for trustworthy retrieval-augmented generation. In *Proceedings of the 2024 Conference on Empirical Methods in Natural Language Processing*, pages 6037–6053, 2024.

[26] H. Qian, Z. Liu, K. Mao, Y. Zhou, and Z. Dou. Grounding language model with chunking-free in-context retrieval. In *Proceedings of the 62nd Annual Meeting of the Association for Computational Linguistics (Volume 1: Long Papers)*, pages 1298–1311, 2024.

[27] A. Slobodkin, E. Hirsch, A. Cattan, T. Schuster, and I. Dagan. Attribute first, then generate: Locally-attributable grounded text generation. In *Proceedings of the 62nd Annual Meeting of the Association for Computational Linguistics (Volume 1: Long Papers)*, pages 3309–3344, 2024.

[28] M. Song, S. H. Sim, R. Bhardwaj, H. L. Chieu, N. Majumder, and S. Poria. Measuring and enhancing trustworthiness of LLMs in RAG through grounded attributions and learning to refuse. In *The Thirteenth International Conference on Learning Representations*, 2025.

[29] Z. Sun, X. Zang, K. Zheng, J. Xu, X. Zhang, W. Yu, Y. Song, and H. Li. RedeEP: Detecting hallucination in retrieval-augmented generation via mechanistic interpretability. In *The Thirteenth International Conference on Learning Representations*, 2025.

[30] G. Team, M. Riviere, S. Pathak, P. G. Sessa, C. Hardin, S. Bhupatiraju, L. Hussenot, T. Mesnard, B. Shahriari, A. Ramé, et al. Gemma 2: Improving open language models at a practical size. *arXiv preprint arXiv:2408.00118*, 2024.

[31] H. Trivedi, N. Balasubramanian, T. Khot, and A. Sabharwal. Musique: Multihop questions via single-hop question composition. *Transactions of the Association for Computational Linguistics*, 10:539–554, 2022.

[32] A. Vaswani, N. Shazeer, N. Parmar, J. Uszkoreit, L. Jones, A. N. Gomez, Ł. Kaiser, and I. Polosukhin. Attention is all you need. *Advances in neural information processing systems*, 30, 2017.

[33] R. Wang, P. Wirawarn, O. Khattab, N. Goodman, and D. Demszky. Backtracing: Retrieving the cause of the query. In *Findings of the Association for Computational Linguistics: EACL 2024*, pages 722–735, 2024.

[34] Z. Wang, H. Zhang, X. Li, K.-H. Huang, C. Han, S. Ji, S. M. Kakade, H. Peng, and H. Ji. Eliminating position bias of language models: A mechanistic approach. In *The Thirteenth International Conference on Learning Representations*, 2025.

[35] S. Wiegreffe, O. Tafjord, Y. Belinkov, H. Hajishirzi, and A. Sabharwal. Answer, assemble, ace: Understanding how LMs answer multiple choice questions. In *The Thirteenth International Conference on Learning Representations*, 2025.

[36] T. Worledge, J. H. Shen, N. Meister, C. Winston, and C. Guestrin. Unifying corroborative and contributive attributions in large language models. In *2024 IEEE Conference on Secure and Trustworthy Machine Learning (SatML)*, pages 665–683. IEEE, 2024.

[37] W. Wu, Y. Wang, G. Xiao, H. Peng, and Y. Fu. Retrieval head mechanistically explains long-context factuality. In *The Thirteenth International Conference on Learning Representations*, 2025.

[38] Z. Wu, X. V. Yu, D. Yogatama, J. Lu, and Y. Kim. The semantic hub hypothesis: Language models share semantic representations across languages and modalities. In *The Thirteenth International Conference on Learning Representations*, 2025.

[39] A. Yang, B. Yang, B. Zhang, B. Hui, B. Zheng, B. Yu, C. Li, D. Liu, F. Huang, H. Wei, et al. Qwen2. 5 technical report. *arXiv preprint arXiv:2412.15115*, 2024.

[40] Z. Yang, P. Qi, S. Zhang, Y. Bengio, W. Cohen, R. Salakhutdinov, and C. D. Manning. Hotpotqa: A dataset for diverse, explainable multi-hop question answering. In *Proceedings of the 2018 Conference on Empirical Methods in Natural Language Processing*, pages 2369–2380, 2018.

[41] X. Ye, R. Sun, S. Arik, and T. Pfister. Effective large language model adaptation for improved grounding and citation generation. In *Proceedings of the 2024 Conference of the North American Chapter of the Association for Computational Linguistics: Human Language Technologies (Volume 1: Long Papers)*, pages 6237–6251, 2024.

[42] X. Yue, B. Wang, Z. Chen, K. Zhang, Y. Su, and H. Sun. Automatic evaluation of attribution by large language models. In *Findings of the Association for Computational Linguistics: EMNLP 2023*, pages 4615–4635, 2023.

[43] Z. Yue, H. Zhuang, A. Bai, K. Hui, R. Jagerman, H. Zeng, Z. Qin, D. Wang, X. Wang, and M. Bendersky. Inference scaling for long-context retrieval augmented generation. In *The Thirteenth International Conference on Learning Representations*, 2025.

[44] M. Yuksekgonul, V. Chandrasekaran, E. Jones, S. Gunasekar, R. Naik, H. Palangi, E. Kamar, and B. Nushi. Attention satisfies: A constraint-satisfaction lens on factual errors of language models. In *The Twelfth International Conference on Learning Representations*, 2024.

A Appendix

B Broad Impact

RAG systems underpin a wide range of everyday activities, from itinerary planning and news aggregation to document drafting, by combining LLMs reasoning with evidence retrieved from external sources. Yet, the practical value of these systems hinges on our ability to verify that each generated statement is genuinely grounded in the retrieved material. The proposed *post-hoc* ARC-JSD method offers a lightweight, modular solution to this problem. Because ARC-JSD can be seamlessly integrated into any open-source RAG pipeline, it provides developers and researchers with an immediate way of auditing attribution fidelity, thereby strengthening the transparency, reliability, and ultimately the public trust in RAG-based applications.

C Limitations

Our work focuses on the analysis to (i) identify the context sentences that most strongly influence a RAG model’s output and (ii) attribute that influence to specific attention heads and MLP layers via a JSD-based metric. Two important directions, therefore, remain unexplored. First, our layer-level view does not reveal which individual neurons within the MLPs mediate context attribution; techniques such as sparse autoencoder (SAE) probing could provide the necessary resolution. Second, we have not yet examined whether our proposed ARC-JSD method as a tool can be generalised to other tasks, such as membership inference attack. This is an exciting direction if the JSD attribution score can be used to locate which data is seen during training.

D Details of the Internal Mechanisms of LLMs

We consider the standard *autoregressive Transformer* architecture used in LLMs, originally introduced by [32] and subsequently analysed in a series of mechanistic studies [13, 8, 12, 7, 20, 21, 44]. Given a prompt of length T , the input tokens (t_1, \dots, t_T) from the context-query pair, each drawn from a vocabulary \mathcal{V} , are mapped to d -dimensional embedding vectors $\mathbf{x}_i^0 \in \mathbb{R}^d$, where the embedding matrix $W_E \in \mathbb{R}^{|\mathcal{V}| \times d}$.

LLMs normally comprise L identical layers. At layer ℓ , the residual stream $\mathbf{X}^\ell = (\mathbf{x}_1^\ell, \dots, \mathbf{x}_T^\ell)$, $\mathbf{x}_i^\ell \in \mathbb{R}^d$, acts as a common read–write buffer for both the multi–head attention and the MLP block [8]. For each token i , the residual update is

$$\mathbf{x}_i^\ell = \mathbf{x}_i^{\ell-1} + \mathbf{a}_i^\ell + \mathbf{m}_i^\ell, \quad (8)$$

where \mathbf{a}_i^ℓ and \mathbf{m}_i^ℓ denote the contributions of the attention and MLP sub-modules, respectively.⁶

After the final layer, a LayerNorm $\sigma(\cdot)$ and the unembedding matrix $W_U \in \mathbb{R}^{d \times |\mathcal{V}|}$ produce the next-token distribution

$$\mathcal{P}_{\text{LM}}(t_{T+1} \mid t_{1:T}) = \text{softmax}(W_U \sigma(\mathbf{x}_T^L)). \quad (9)$$

Each layer contains H attention heads, each factorised into QK and OV circuits operating with weight matrices $W_Q^{\ell,h}, W_K^{\ell,h}, W_V^{\ell,h}, W_O^{\ell,h} \in \mathbb{R}^{d \times d}$. The QK circuit establishes the attention pattern $A^{\ell,h} \in \mathbb{R}^{T \times T}$, while the OV circuit transports content across sequence positions. For head h the contribution of source token j to target token i is

$$\mathbf{a}_{i,j}^{\ell,h} = A_{i,j}^{\ell,h} (\mathbf{x}_j^{\ell-1} W_V^{\ell,h}) W_O^{\ell,h}, \quad (10)$$

and the total attention update for token i is

$$\mathbf{a}_i^\ell = \sum_{h=1}^H \sum_{j=1}^T \mathbf{a}_{i,j}^{\ell,h}. \quad (3)$$

A concise per-head summary is $\mathbf{a}_i^{\ell,h} = \sum_j \mathbf{a}_{i,j}^{\ell,h}$.

Following the key–value interpretation of MLP layers [13, 8], let $W_{\text{in}}^\ell \in \mathbb{R}^{d_{\text{m}} \times d}$ and $W_{\text{out}}^\ell \in \mathbb{R}^{d \times d_{\text{m}}}$ denote the input and output weights. Given $\mathbf{x}_i^{\ell-1}$, the block first produces coefficients

$$\mathbf{k}_i^\ell = \gamma(W_{\text{in}}^\ell \mathbf{x}_i^{\ell-1}) \in \mathbb{R}^{d_{\text{m}}}, \quad (11)$$

where γ is the activation function (e.g. GELU). These coefficients weight the value vectors (rows of W_{out}^ℓ) to yield

$$\mathbf{m}_i^\ell = \sum_{n=1}^{d_{\text{m}}} \mathbf{k}_i^{\ell,n} \mathbf{v}^{\ell,n}, \quad \mathbf{v}^{\ell,n} \equiv W_{\text{out}}^\ell[n, :]. \quad (12)$$

E Experimental Details

We run all experiments using H100 GPUs, and we use the sentence tokeniser from the *nltk* library [1] to preprocess all datasets. For all RAG models, i.e., Qwen2-1.5B-Instruct, Qwen2-7B-Instruct [39], Gemma2-2B-Instruct and Gemma2-9B-Instruct [30], we use their standard chat templates to construct the prompt, i.e., using the context and query as a user’s message.

When constructing prompts for TyDi QA dataset, we follow the prompt:

Context: {context}

Query: {question}

⁶Layer normalisation preceding each sub-module is omitted here for clarity.

For Hotpot QA and MuSiQue datasets which have multiple documents for each data sample, the prompt is constructed as:

```

Title: {title_1}
Content: {document_1}
...
Title: {title_n}
Content: {document_n}

Query: {question}

```

F GPT-4.1 as Judge for Comparison between Generated Responses of RAG models and Gold Answers from Datasets

After using our ARC-JSD to correctly locate the top relevant context sentences for generated responses, we further utilise GPT4.1 as a judge to check whether those responses correctly answer queries based on the corresponding context. As Table 6 shows, generated responses from all RAG models achieve high accuracy in successfully answering the queries based on the contexts, which demonstrates the fundamental ability of those instructed RAG models.

Table 6: GPT4.1 as a judge to evaluate the semantic equivalence between generated responses of RAG models and the corresponding gold answers from those datasets.

Acc. (%)	Qwen2-1.5B-IT	Qwen2-7B-IT	Gemma2-2B-IT	Gemma2-9B-IT
TyDi QA	99.1	99.4	98.9	99.5
Hotpot QA	99.2	99.5	99.1	99.6
MuSiQue	99.3	99.4	99.2	99.8

G Compute-accuracy Trade-off Between Different Baselines and Our ARC-JSD

We mainly compare the compute-accuracy trade-off between different baselines and our proposed ARC-JSD when attributing responses to relevant context. As Figure 5 and 6 show, our ARC-JSD method can achieve up to 3-fold speedup compared to other baselines. In addition, ARC-JSD is consistently Pareto-optimal over different LLM backbone sizes.

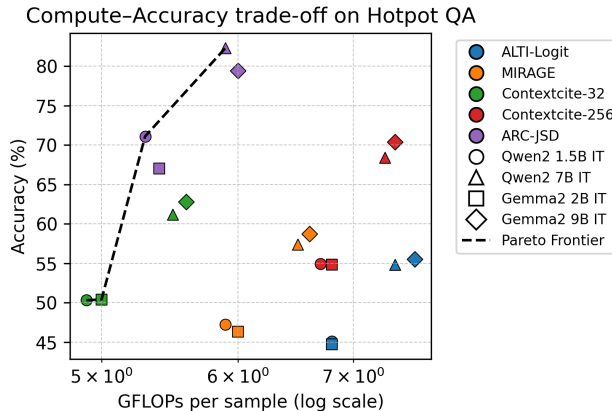


Figure 5: The compute-accuracy trade-off on Hotpot QA dataset for 4 baselines and ARC-JSD on 4 LLM backbones

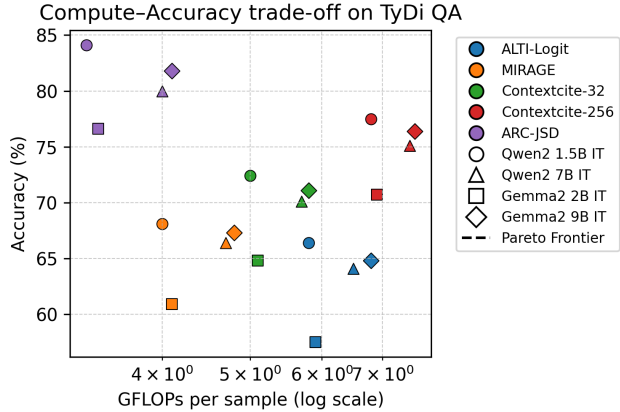


Figure 6: The compute-accuracy trade-off on TyDi QA dataset for 4 baselines and ARC-JSD on 4 LLM backbones

H Examples of ARC-JSD Context Attribution

We demonstrate more examples of our ARC-JSD attribution method used for different RAG models on different datasets, where each example includes the query, generated responses and located top-1 sentence from the context.

Example of ARC-JSD attributions for Qwen2-1.5B-IT on TyDi QA

Query

How many wings does a mosquito have?

Response (attributed statement is highlighted)

A mosquito has two wings.

attribution

Top-1 Source (from the context)

... The word “mosquito” (formed by *mosca* and diminutive *-ito*)[2] is Spanish for “little fly”. [3] **Mosquitoes have a slender segmented body, a pair of wings, three pairs of long hair-like legs, feathery antennae, and elongated mouthparts.**

Example of ARC-JSD attributions for Qwen2-7B-IT on MuSiQue

Query

What is the date of birth of the person who was part of Ratata?

Response (attributed statement is highlighted)

The date of birth for Mauro Scocco, who was part of the pop group Ratata, is given as September 11, 1962.

attribution

Top-1 Source (from the context)

... His mother's name was not recorded in history. Title: Mauro Scocco
Mauro Scocco (born 11 September 1962) is a Swedish pop artist of Italian descent.
He has been described as "one of the sharpest songwriters in Sweden". ...

Example of ARC-JSD attributions for Gemma2-2B-IT on TyDi QA

Query

When was the friends song was released which is taken from the fourth studio album of canadian singer and song writer Justin Bieber?

Response (attributed statement is highlighted)

The song "Friends" was released on ****August 17, 2017****. It's important to note that this is from Justin Bieber's fourth studio album, "Purpose".

attribution

Top-1 Source (from the context)

... It was written by Bieber, Julia Michaels, Justin Tranter and BloodPop, with production handled by BloodPop. **The song was released through GENPOP Corporation, RBMG Records, School Boy Records, Def Jam Recordings and Republic Records on August 17, 2017**. It is Bieber's first single credited as lead artist to be released in over a year, the previous being "Company", which was released in March 2016 for his studio album "Purpose" (2015). ...

Example of ARC-JSD attributions for Gemma2-9B-IT on Hotpot QA

Query

Tom Thumb Food & Pharmacy is part of the southern division of a grocery company based in what city?

Response (attributed statement is highlighted)

The answer is **Boise, Idaho**. The text states that Tom Thumb Food & Pharmacy is part of the Southern division of Albertsons, and Albertsons Companies LLC is based in Boise, Idaho.

attribution

Top-1 Source (from the context)

... It is also known in Brazil as "Chapolin", "Vermelhinho" ("Little Red One") and "Polegar Vermelho" ("Red Thumb") in allusion to the famous fairy tale character Tom Thumb. Title: Albertsons **Albertsons Companies LLC is an American grocery company founded and based in Boise, Idaho**. It is privately owned and operated by investors, including Cerberus Capital Management.

I JSD-based Mechanistic Insights for Located Attention Heads and MLPs

We visualise more attention heads and MLP heatmaps using our JSD-based mechanistic approach, where we can find that most RAG models include attribution-relevant attention heads and MLPs across the intermediate and higher layers. On the Hotpot QA and MuSiQue datasets, Gemma2-2B-IT has some relevant attention heads on the lower layers.

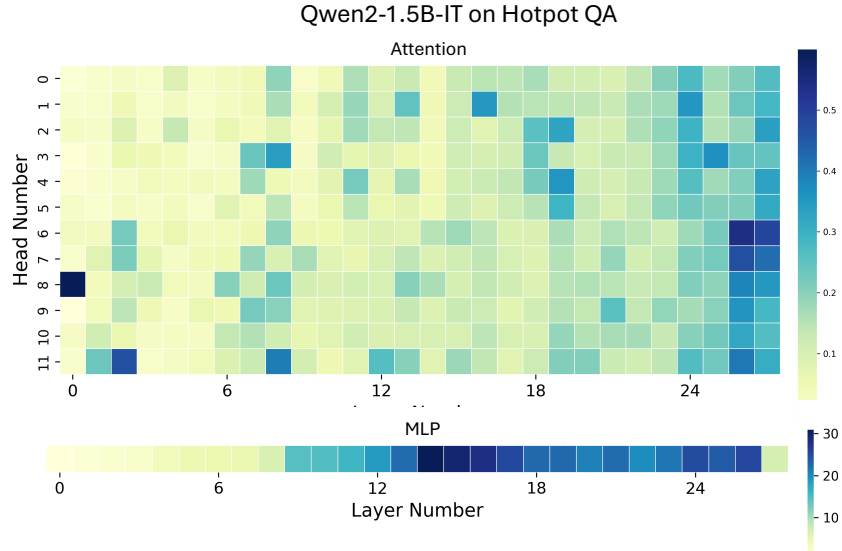


Figure 7: The average JSD score of attention heads and MLP of Qwen2-1.5B-IT on Hotpot QA dataset across all layers. The deeper colour indicates larger JSD scores.

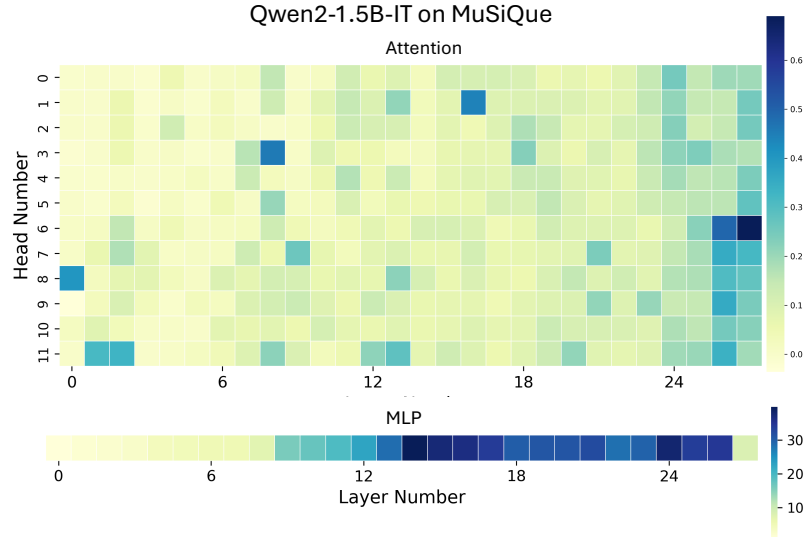


Figure 8: The average JSD score of attention heads and MLP of Qwen2-1.5B-IT on MuSiQue dataset across all layers. The deeper colour indicates larger JSD scores.

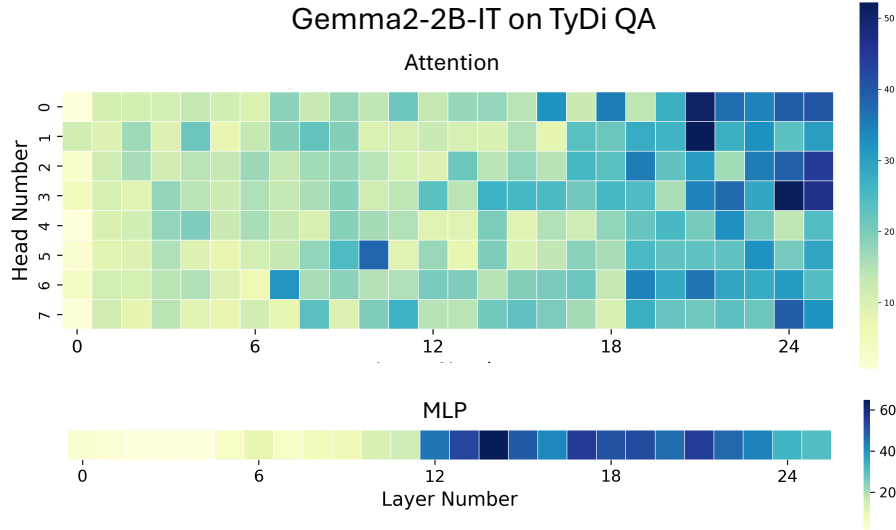


Figure 9: The average JSD score of attention heads and MLP of Gemma2-2B-IT on TyDi QA dataset across all layers. The deeper colour indicates larger JSD scores.

J Comparisons of JSD with KL, Wasserstein, TV and MMD in Detail

Direct log-probability or KL Divergence. Most existing baselines, e.g., ContextCite [6], Self-Cite [3] and AttriBoT [19], use direct log-probability or KL divergence as metric for context attribution. However, these metrics drop diverges if the masked run assigns ≈ 0 probability to the token, which is sensitive to highly-skewed token frequencies. Moreover, if JSD is replaced with KL in the Eq. 1 and Eq. 2, it will bring some influence to the attribution impact:

- **Asymmetry / direction choice:** We must choose $\text{KL}(P|Q)$ or $\text{KL}(Q|P)$. The ranking of sentences can flip depending on direction. There is no principled reason to prefer one for attribution. Using the symmetrized Jeffreys divergence $\text{KL}(P|Q) + \text{KL}(Q|P)$ removes directionality, but it does not

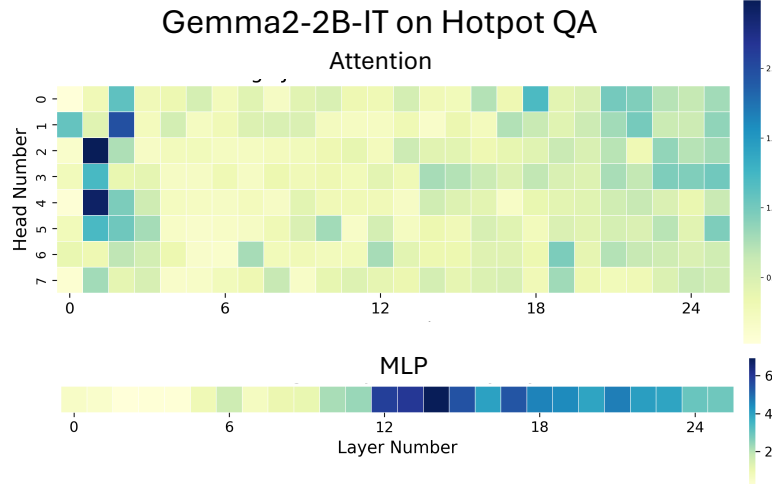


Figure 10: The average JSD score of attention heads and MLP of Gemma2-2B-IT on Hotpot QA dataset across all layers. The deeper colour indicates larger JSD scores.

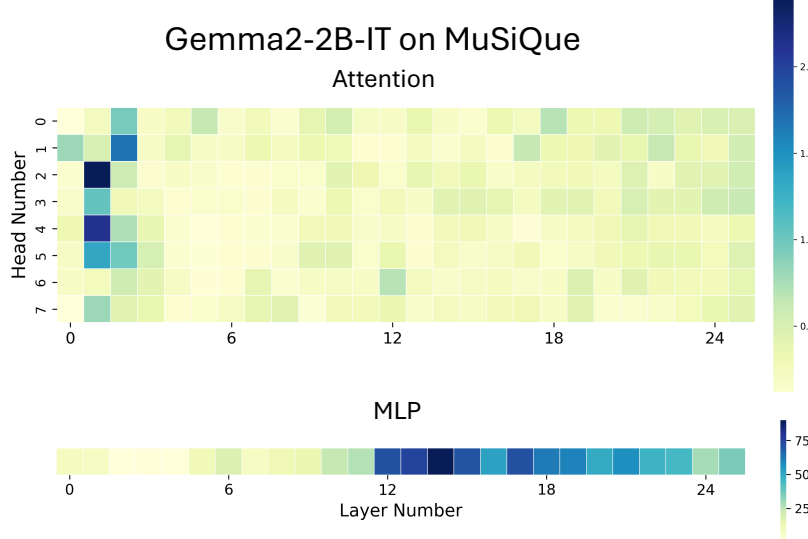


Figure 11: The average JSD score of attention heads and MLP of Gemma2-2B-IT on MuSiQue dataset across all layers. The deeper colour indicates larger JSD scores.

fix the core issues, such as unboundedness, tail sensitivity, numerical instability, and lack of a common scale.

- **Unbounded & numerically unstable:** If the ablated run puts (near) zero mass on a token that the full run assigns mass to (that is common at deeper layers), KL explodes or becomes extremely noisy unless we add ad-hoc smoothing. However, this tends to overweight tail events and can produce false positives.
- **Cross-layer incomparability:** Because KL or Jeffreys are unbounded, a few positions with tiny denominators dominate the sentence score, i.e., comparing “how much layer 7 changed” vs “layer 28” becomes unstable. JSD’s boundedness is crucial for consistent ranking and aggregation.

Therefore, if we replace JSD with KL, there will be lower precision/recall for “relevant sentence” ranking (it brings more variance, dependence on ε and direction), which will further lead to low

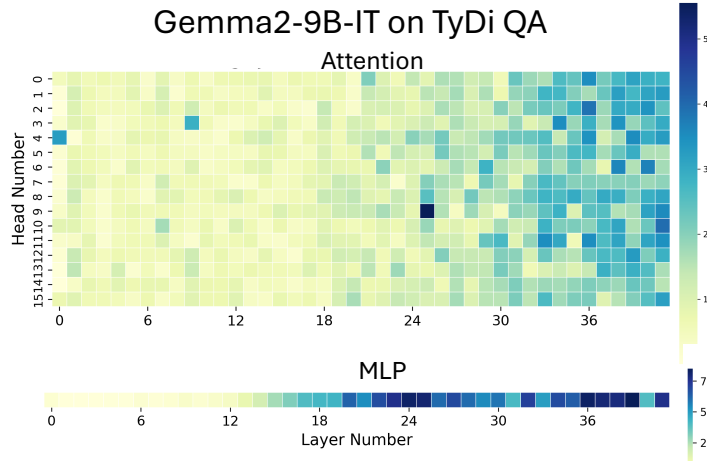


Figure 12: The average JSD score of attention heads and MLP of Gemma2-9B-IT on TyDi dataset across all layers. The deeper colour indicates larger JSD scores.

attribution accuracy. It will also tend to disagree more with independent, behaviour-aligned probes (e.g., semantic gain used in our work), although KL divergence has the same FLOPs as JSD.

Wasserstein Distance. Assume we choose a ground metric $c(a, b)$ over tokens (e.g., token-Hamming, character edit distance, or embedding-cosine cost), and use entropic-regularised Sinkhorn for Wasserstein. When we replace JSD with Wasserstein distance, it will affect attribution:

- **Metric choice drives the result:** Edit distance and embedding-cosine will encode orthography or static similarity, not decoding behaviour. They may call a move toward a typo-like token “cheap” and a move toward a semantically correct rival “expensive”, which misaligns with which changes actually flip the output (See more detailed discussion below).
- **Hyperparameters matter:** Sinkhorn ε (regularisation) and number of iterations change the scale and ranking. Different reasonable settings can reorder “relevant sentences”.
- **Context dependence missing:** A single cost matrix $c(a, b)$ ignores that token meaning is position- and layer-dependent in a transformer-based LLM, which means that we either accept a mismatch or introduce layer-specific cost matrices (which becomes circular and heavy).

So, rankings become sensitive to modelling choices not tied to the LM’s probability geometry, typically reducing correlation with behaviour (semantic gain) and causal precision in context attribution.

For FLOPs comparison, if we use full support for Wasserstein distance, Sinkhorn per pair costs $O(KV^2)$ operations (and $O(V^2)$ memory) for K iterations, where $V \sim 152k$. Instead, if we use top- k support trick, we restrict to top- k tokens of P and Q (say $k \in [100, 500]$). Cost becomes $O(Kk^2)$ per $(layer, r_j)$, plus top- k selection $O(Vlogk)$. This is still orders of magnitude above JSD in practice and adds hyperparameters k, K, ε .

MMD Metric. Let $k(\cdot, \cdot)$ be a kernel on tokens; for categorical distributions one computes $MMD^2(P, Q) = (P - Q)^\top K(P - Q)$ with $K_{ab} = k(a, b)$. When we replace JSD with MMD, it will affect attribution:

- **Kernel choice = modelling assumption:** We need to make multiple choices: Gaussian or Laplace on which embeddings? What bandwidth? Results (and rankings) will vary with these choices.
- **Units & interpretability:** Values depend on kernel scale and there is no direct link to entropy or cross-entropy (which govern decoding). The equal mass moves on tail tokens can dominate if the kernel puts them in “diverse” regions, even though they don’t affect behaviour.
- **Edge case:** If we set $k(a, b) = \mathbf{1}[a=b]$, MMD reduces to ℓ_2 on probabilities, again misaligned with decoding (uniformly weights all coordinates).

So, replacing JSD with MMD will bring more sensitivity to hyperparameters, and it has weaker correlation with behaviour, and less stable cross-layer comparisons than JSD.

For FLOPs comparison, if we use dense kernel, a naive computation is $O(V^2)$ per (layer, r_j) (matrix–vector with $K \in \mathbb{R}^{V \times V}$). Instead, if we use Low-rank/Nyström rank r , it will cost $O(rV)$ per pair, but we must tune r and store factors. With $r = 256$, this is $\sim 256 \times$ the work of JSD’s $O(V)$ reduction, and quality also depends on r . We also need to consider plus kernel selection/bandwidth tuning overhead.

Using edit distance or embedding cosine as metrics for Wasserstein or MMD. When Wasserstein or MMD uses edit distance or embedding cosine as metrics, it has several limitations:

1. Edit distance (token/character level):

- **Tokenisation mismatch:** In subword vocabularies, a single semantic change can span many subwords, and edit distance on token strings becomes an artefact of the tokeniser, not semantics.
- **Semantic blindness:** For the example: “Paris” \rightarrow “Lyon” (same POS, both cities) and “Paris” \rightarrow “Party”. At the token level, any substitution has unit cost, so replacing “Paris” with either “Lyon” or “Party” is equally cheap, despite radically different semantic consequences. With subword tokenisation, the cost becomes tokeniser-dependent. Character-level edit distance differentiates orthography (e.g., “Party” is closer to “Paris” than “Lyon”), which misaligns with factual attribution
- **Decoding irrelevance:** The decoder’s choice is driven by probability mass, not string operations. A small edit distance can correspond to a huge shift in probability, and vice versa.

2. Embedding-cosine ground metrics:

- **Context dependence:** Token meaning in transformers is contextual. A static vocab-level embedding (or even the unembedding vectors) is not the representation used at the position/layer where attribution is measured. A faithful ground metric would need position- and layer-specific distances, which will explode in complexity and introduce circularity.
- **Anisotropy & polysemy:** Cosine distances in high-dimensional language embeddings are known to concentrate and to blur senses, which means that “nearby” vectors can still correspond to different factual claims. Wasserstein might then deem a large semantic change “cheap to move,” underestimating its effect on generation.
- **Tunable choices:** Which embedding? Which layer? Do we normalise? Each choice changes the cost matrix and can alter the ranking of “relevant” layers and context sentences, which is exactly the orthogonal modelling assumption we seek to avoid.

TV Metric. Here, we provide a simple example to explain why TV distance is not an ideal metric to use for context attribution.

The definition of TV distance for two discrete distributions P, Q over the same vocabulary is:

$$\text{TV}(P, Q) = \frac{1}{2} \sum_t |P(t) - Q(t)| \quad (13)$$

Here, TV measures the total amount of probability mass moved, but not where it moved.

For any decoding methods used in LLMs, they are more affected by the position where probability mass moved, e.g., greedy decoding picks the token with the largest probability, or sampling and beam search are also dominated by how mass is distributed among the top few tokens.

Here is one example to consider a single decoding step with three candidate tokens: t_1 = the ground-truth/desired token, t_2 = a strong competitor, t_3 = a low-probability tail token.

Let the full-context distribution at one decoding step be:

$$P = [p(t_1), p(t_2), p(t_3)] = [0.52, 0.43, 0.05] \quad (14)$$

Consider two different ablated distributions that both move the same amount of mass $\varepsilon = 0.05$:

Case A—move mass in the tail (does not flip the output prediction):

Shift ε from t_3 (tail) to t_2 : i.e., $Q_{\text{tail}} = [0.52, 0.48, 0.00]$. TV calculation will be:

$$\text{TV}(P, Q_{\text{tail}}) = \frac{1}{2}(|0.52-0.52| + |0.43-0.48| + |0.05-0.00|) = \frac{1}{2}(0 + 0.05 + 0.05) = 0.05. \quad (15)$$

When we use greedy choice, we still choose t_1 because 0.52 remains the largest.

Case B — move mass off the top onto its nearest competitor (does flip the output prediction):

Shift the same $\varepsilon = 0.05$ from t_1 to t_2 : $Q_{\text{top}} = [0.47, 0.48, 0.05]$. TV calculation will be:

$$\text{TV}(P, Q_{\text{top}}) = \frac{1}{2}(|0.52-0.47| + |0.43-0.48| + |0.05-0.05|) = \frac{1}{2}(0.05 + 0.05 + 0) = 0.05. \quad (16)$$

When we use greedy choice, it will flip to t_2 because $0.48 > 0.47$.

Both perturbations have the same $\text{TV} = 0.05$, but only Case B changes the token the model outputs.

If we move ε probability from any token i to any token j (and leave all others unchanged), the absolute differences are $|- \varepsilon|$ for i , $+\varepsilon|$ for j , and 0 elsewhere, so $\text{TV}(P, Q) = \frac{1}{2}(\varepsilon + \varepsilon) = \varepsilon$, regardless of which tokens i and j you chose. Which means that TV “sees” only the amount moved, not where it came from or went.

Yet output behaviour depends critically on where the mass moves:

- The arg-max flips when $p_j + \varepsilon > p_i - \varepsilon \iff \varepsilon > \frac{1}{2}(p_i - p_j)$. In our numbers, $p_1 - p_2 = 0.09$, so any $\varepsilon > 0.045$ flips the token, where Case B does ($\varepsilon = 0.05$), Case A does not.
- For sampling, the log-odds change by $\Delta \log \frac{p_i}{p_j} = \log \frac{p_i - \varepsilon}{p_j + \varepsilon} - \log \frac{p_i}{p_j}$, which is large and negative only when you move mass between the top competitors (Case B), not when you shuffle tail mass (Case A). But TV assigns both moves the same distance.

In addition, we conduct ablation studies to compare different metrics with JSD on compute-accuracy trade-off on different datasets with 4 LLM backbones. As shown in Fig. 13 and Fig. 14, JSD yields a better compute-accuracy trade-off than other metrics.

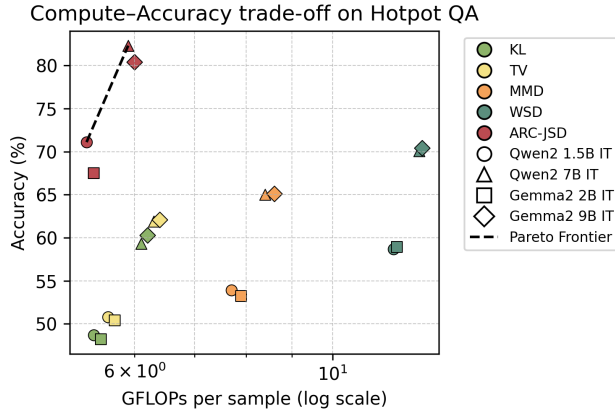


Figure 13: The compute-accuracy trade-off on Hotpot QA for different metrics and ARC-JSD on 4 LLM backbones with GFLOPs \log_{10} scale per sample.

K Case Studies of Attention and MLP’s Contribution for Each Response Token

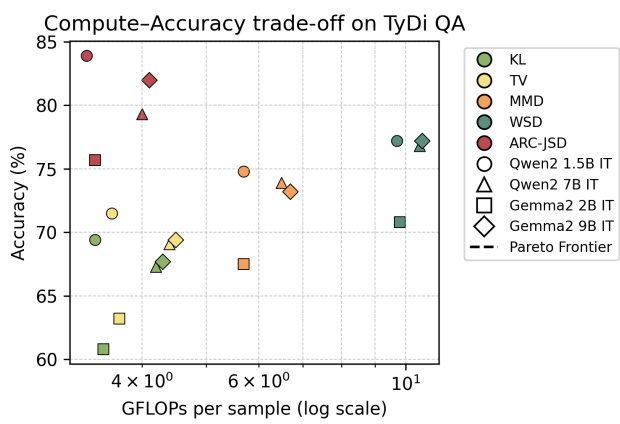


Figure 14: The compute-accuracy trade-off on TyDi QA for different metrics and ARC-JSD on 4 LLM backbones with GFLOPs \log_{10} scale per sample.

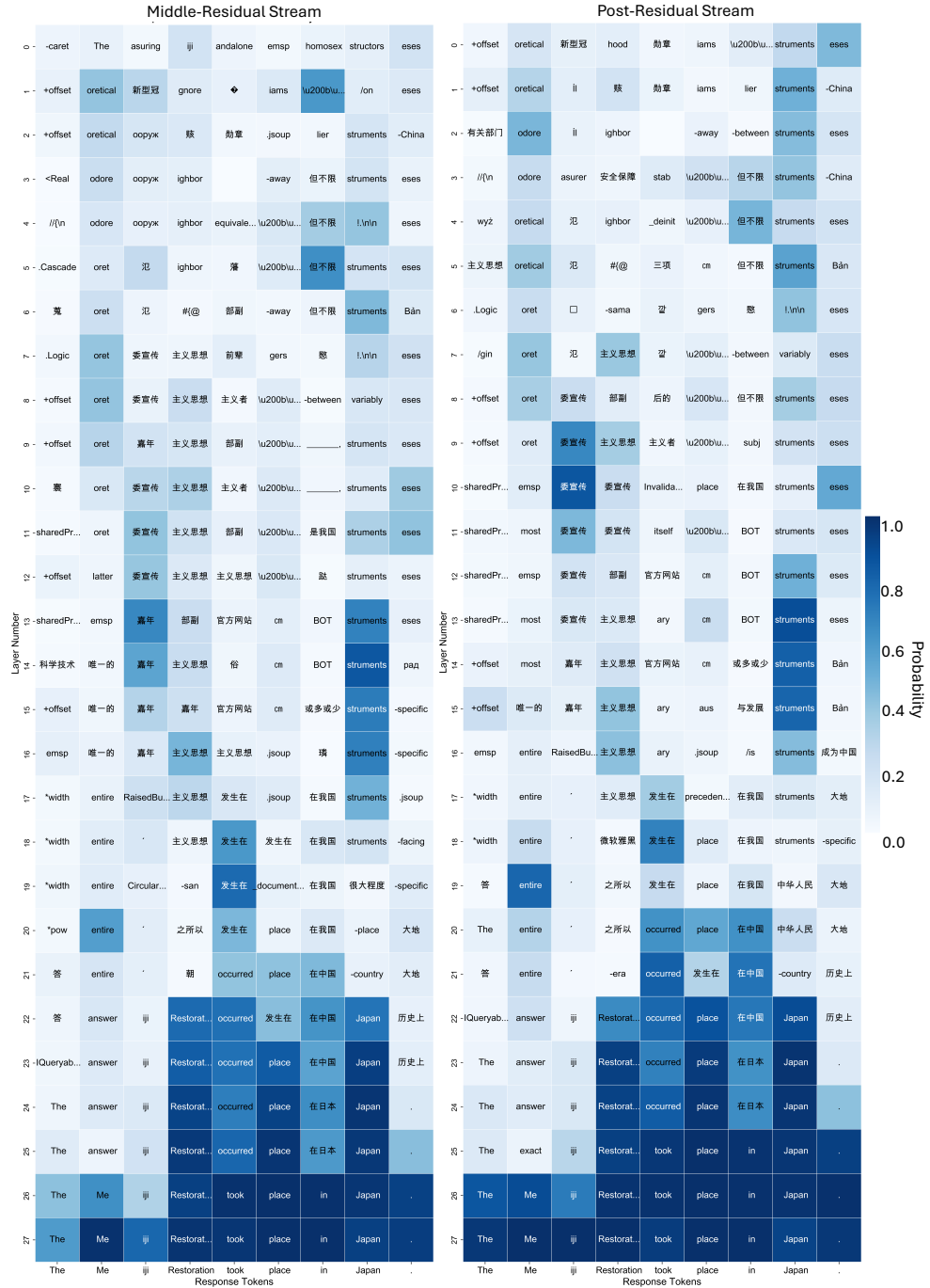


Figure 15: The projection of $\mathbf{x}_i^{\ell, \text{mid}}$ and $\mathbf{x}_i^{\ell, \text{post}}$ via Logit Lens to vocabulary space from layer 20 to layer 27 of Qwen2-1.5B IT in TyDi QA data sample, where the generated response \mathcal{R} is “*The Meiji Restoration took place in Japan.*”. Each cell shows the most probable token decoded via Logit Lens.

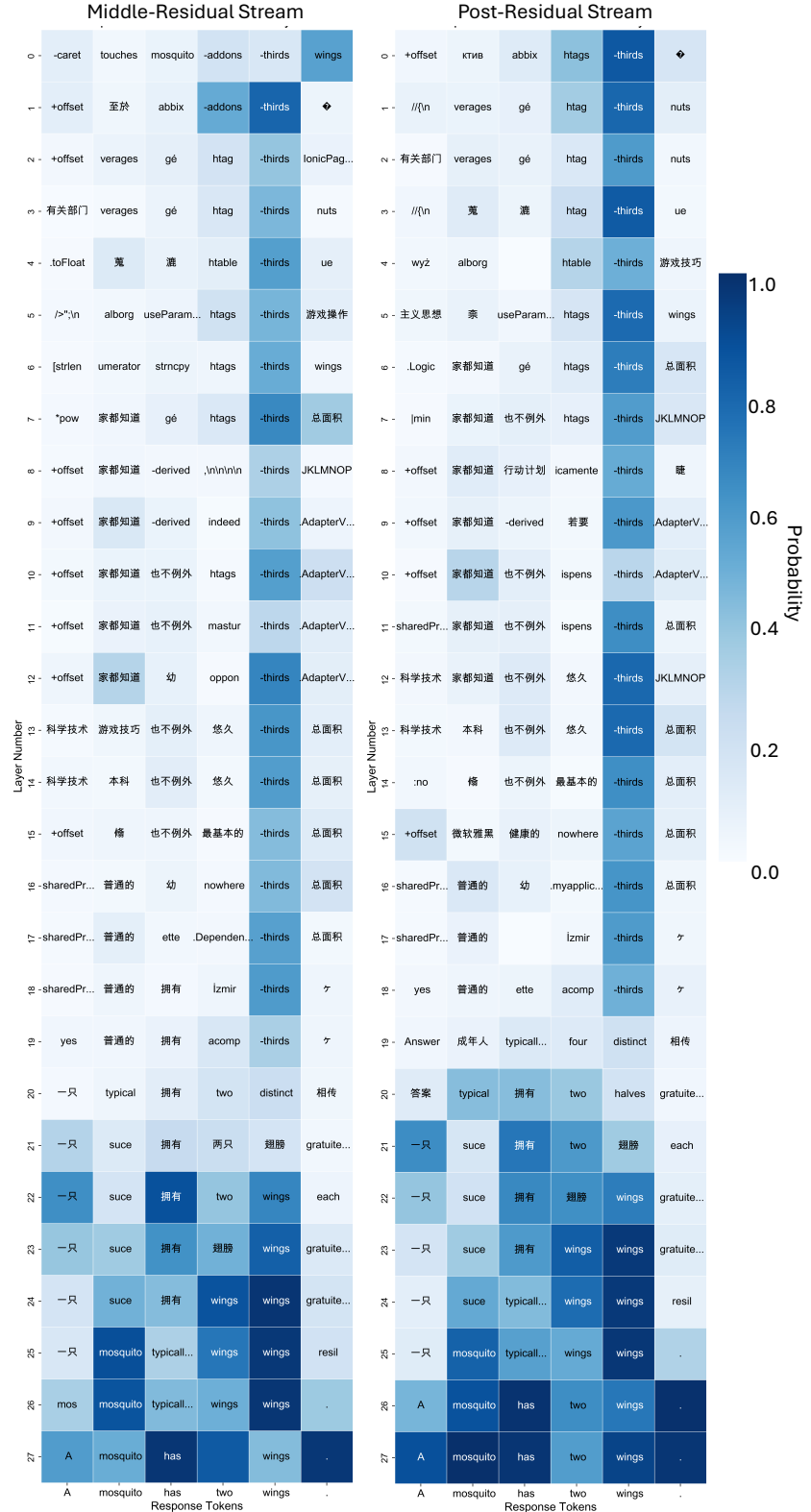


Figure 16: The projection of $\mathbf{x}_i^{\ell, \text{mid}}$ and $\mathbf{x}_i^{\ell, \text{post}}$ via Logit Lens to vocabulary space from layer 20 to layer 27 of Qwen2-1.5B IT in TyDi QA data sample, where the generated response \mathcal{R} is “A mosquito has two wings.”. Each cell shows the most probable token decoded via Logit Lens. The colour indicates the probability of the decoded token of the corresponding $\mathbf{x}_i^{\ell, \text{mid}}$ or $\mathbf{x}_i^{\ell, \text{post}}$.

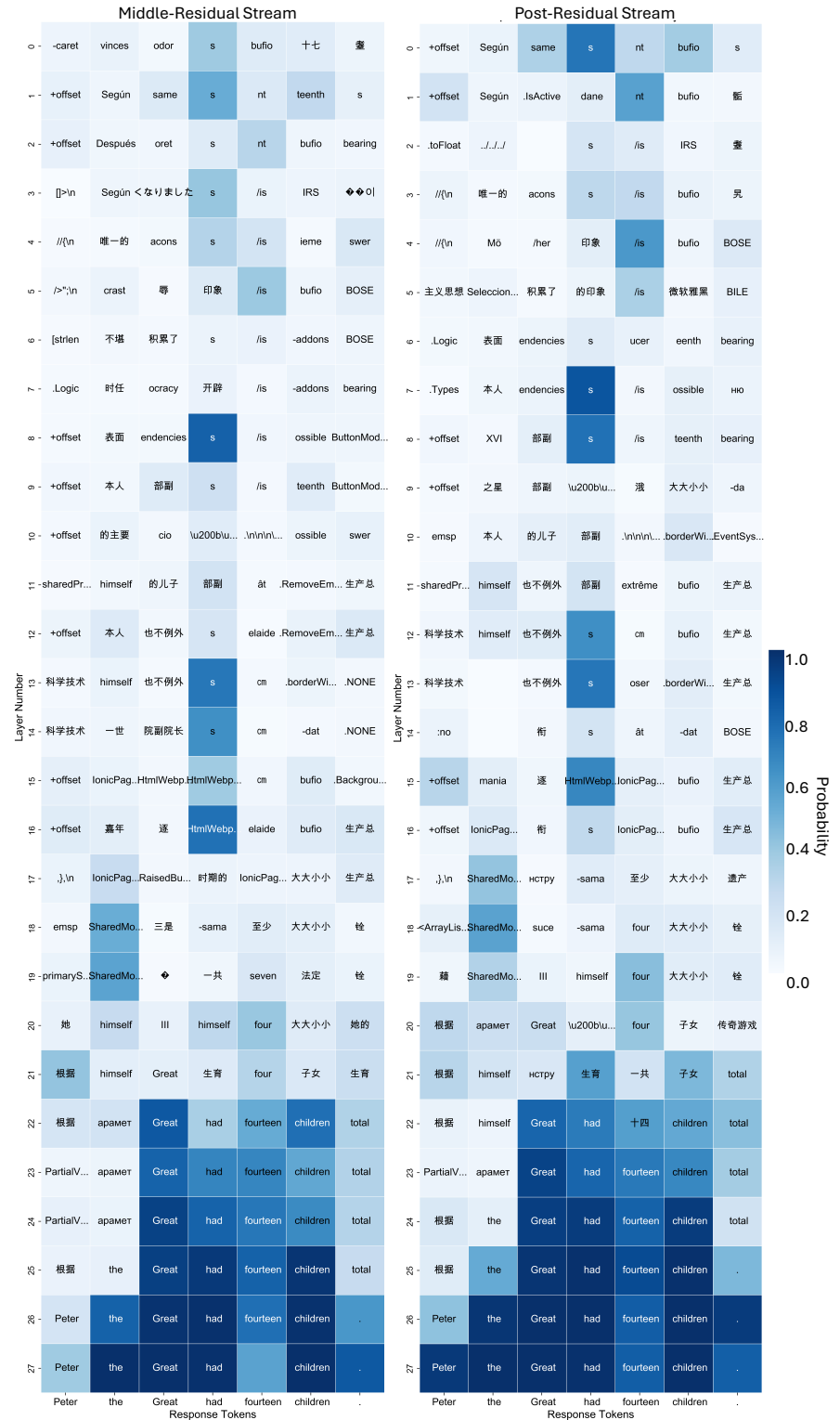


Figure 17: The projection of $x_i^{\ell, \text{mid}}$ and $x_i^{\ell, \text{post}}$ via Logit Lens to vocabulary space from layer 20 to layer 27 of Qwen2-7B IT in TyDi QA data sample, where the generated response \mathcal{R} is “*Peter the Great had fourteen children.*”. Each cell shows the most probable token decoded via Logit Lens.